Synchronization phenomena for a pair of locally coupled chaotic electrochemical oscillators: A survey

M. Rivera and G. Martínez Mekler
Centro de Ciencias Físicas, UNAM, Cuernavaca 62210, Morelos, México

P. Parmananda
Centro de Ciencias Físicas, UNAM, Cuernavaca 62210, Morelos, México
and Facultad de Ciencias, UAEM, Avenida Universidad 1001, Colonia Chamilpa, Cuernavaca, Morelos, México

(Received 30 March 2006; accepted 5 June 2006; published online 27 September 2006)

Chaotic synchronization of two locally coupled electrochemical oscillators is studied numerically. Both bidirectional and unidirectional couplings are considered. For both these coupling scenarios, varying the characteristics of the coupling terms (functional form and/or strength) reveals a wide variety of synchronization phenomena. Standard diagnostic tests are performed to verify and classify the different types of synchronizations observed. © *2006 American Institute of Physics*.
[DOI: 10.1063/1.2218047]

Synchronization is a natural occurrence in an ensemble of coupled oscillators. It plays a crucial role in the collective dynamics exhibited by large populations of such oscillators. The abundance of these ensembles/populations in nature lends the synchronous phenomena a flavor of omnipresence. Synchronization has diverse manifestations depending on the nature of the underlying couplings and system configurations. Moreover, the concept of synchronization, apart from being an interesting dynamical problem, is fundamental for the understanding of numerous physical, chemical, biological, and ecological systems. The first documented experiments reporting synchronization were performed by the famous dutch physicist Huygens using pendulum clocks.

I. INTRODUCTION

Chaotic synchronization, although studied earlier by Yamasha and Fuujisaka[1,2] and by Afraimovich, Verichev, and Rabinovich,[3] was brought to the limelight by the works of Pecora and Carroll.[4,5] Chaotic synchronization, by definition, appears a little counterintuitive since the sensitivity of the chaotic trajectories to small variations in initial conditions seems incompatible with the convergence effect that exemplifies the concept of synchronization. However, it has been categorically demonstrated, both theoretically and experimentally,[6–11] that chaotic systems in the present of suitable external perturbations and/or appropriate mutual interactions are capable of exhibiting different kinds of synchronization behavior. A number of recent books[12–14] and a comprehensive review article[15] furnish an up-to-date account of the efforts invested and the advances achieved in the field of synchronization.

Interest in the investigation of electrochemical oscillations has been enhanced due to the advances made in the field of nonlinear dynamics. This is in part due to the wide variety of nonlinear behavior that these systems exhibit, making them an ideal playground for chaoticians. Furthermore, they posses other favorable attributes such as (a) they are easy and relatively cheap to assemble and (b) that the experimental dynamics are fairly reproducible. Oscillations have been observed and characterized in several electrochemical processes involving the electrodissolution of metals, including both anodic and cathodic reactions under potentiostatic and galvanostatic conditions.[16–20] Most of these electrochemical systems exhibit behavior typical of nonlinear deterministic systems. This includes spontaneous oscillations, period doubling, mixed mode dynamics, multistability, and the existence of deterministic chaos.

The transport of chemical species is the most natural way that coupling emerges between electrochemical oscillators. The overlap of potential fields is another one of the frequent sources of coupling in these systems. The synchronization of electrochemical oscillators has been studied extensively by the group of Hudson and collaborators at the University of Virginia. Using experiments with two or more electrochemical oscillators, coupled globally, they have verified the existence of different types of chaotic synchronization.[21–23] Moreover, they have studied the collective behavior exhibited by a population of these oscillators.[24,25] In almost all their experiments involving chaotic synchronization, the global coupling between the electrodes is in conjunction with a set of series and/or parallel external resistors. In contrast, here we study, numerically, the different types of synchronization phenomena observed when two chaotic electrochemical oscillators are coupled locally. Both unidirectional and bidirectional coupling scenarios are considered. The paper is organized as follows: In the following section, we present the numerical electrochemical model used to study the diverse synchronization effects. In Sec. III, results involving distinct types of synchronization for a bidirectional coupling are furnished. The different domains of synchronization for a unidirectional coupling scenario are characterized and classified in Sec. IV. This includes an elegant strategy to augment the efficiency

and consequently the utility of anticipation synchronization. Finally, a brief recap of the obtained results is presented as conclusions in Sec. V.

II. NUMERICAL MODEL

We look for chaotic synchronization in a model for aqueous electrochemical corrosion[26,27] described by three dimensionless coupled ordinary differential equations:

$$\dot{Y} = p(1 - \theta_{OH} - \theta_O) - qY, \tag{1}$$

$$\dot{\theta}_{OH} = Y(1 - \theta_{OH} - \theta_O) - [\exp(-\beta\theta_{OH}) + r]\theta_{OH} + 2s\theta_O(1 - \theta_{OH} - \theta_O), \tag{2}$$

$$\dot{\theta}_O = r\theta_{OH} - s\theta_O(1 - \theta_{OH} - \theta_O). \tag{3}$$

The variables θ_O and θ_{OH} represent the fraction of the electrode surface covered by two different chemical species, while Y represents the concentration of metal ions in the electrolytic solution. The system parameters p, q, r, s, and β are determined by chemical reaction rates in the model. This set of ordinary differential equations is integrated using a fourth order Runge-Kutta algorithm. Previous numerical studies have shown that, depending on the parameter values, this model may exhibit simple periodic oscillations, bistability, mixed mode behavior, and period doubling cascade leading up to chaotic dynamics.[27] The model system exhibits deterministic chaos for the parameter set $\{p, q, r, s, \beta\}$ at $\{2.0\times10^{-4}, 1.0\times10^{-3}, 2.0\times10^{-5}, 9.7\times10^{-5}, 5.0\}$. To study the different types of chaotic synchronizations, two copies of the model system are constructed. This set of ordinary differential equations is subsequently coupled appropriately in both the unidirectional and the bidirectional sense.

III. CHAOTIC SYNCHRONIZATION UNDER BIDIRECTIONAL COUPLING

In this section, we present three different synchronization effects observed when two nonidentical (small parameter mismatch) electrochemical oscillators are subjected to symmetric bidirectional coupling. The model equations, subsequent to the incorporation of the coupling terms, have the following form:

$$\dot{Y}^{1,2} = \omega^{1,2}[p(1 - \theta_{OH}^{1,2} - \theta_O^{1,2}) - qY^{1,2}] + \epsilon(Y^{2,1} - Y^{1,2}), \tag{4}$$

$$\dot{\theta}_{OH}^{1,2} = \omega^{1,2}[Y^{1,2}(1 - \theta_{OH}^{1,2} - \theta_O^{1,2}) - [\exp(-\beta\theta_{OH}^{1,2}) + r]\theta_{OH}^{1,2} + 2s\theta_O^{1,2}(1 - \theta_{OH}^{1,2} - \theta_O^{1,2})] + \epsilon(\theta_{OH}^{2,1} - \theta_{OH}^{1,2}), \tag{5}$$

$$\dot{\theta}_O^{1,2} = r\theta_{OH}^{1,2} - s\theta_O^{1,2}(1 - \theta_{OH}^{1,2} - \theta_O^{1,2}) + \epsilon(\theta_O^{2,1} - \theta_O^{1,2}). \tag{6}$$

The indices (1, 2) in the superscripts of Eq. (4)–Eq. (6) correspond to the two chaotic oscillators. The bidirectional coupling terms are introduced in all three evolution equations. Subsequently, the coupling constant ϵ is monotonically varied (increased) to explore the different domains of chaotic synchronization. The parameter sets are chosen such that each individual oscillator exhibits chaotic behavior. A parameter mismatch (ω) between the two oscillators is intentionally introduced. This parameter mismatch is indispensable for the observation of bidirectional lag synchronization,[28,29] which involves a constant time lag (τ) between the dynamics of the two oscillators. However, our numerical results indicate that the existence of a parameter mismatch is not a sufficient condition for observing the elusive lag synchronization. Figure 1 depicts the times between successive maximas (ΔT) as a function of the parameter mismatch ω for our uncoupled (single oscillator; $\epsilon=0$) numerical system. The solid line corresponds to the average ΔT of this distribution for the underlying chaotic attractor. For this discernible change in the average ΔT value, our model system could exhibit lag synchronization, but only for some appropriate values of the parameters. This led us to conclude that the existence of parameter mismatch, is a necessary but not a sufficient condition for the emergence of lag synchronization.

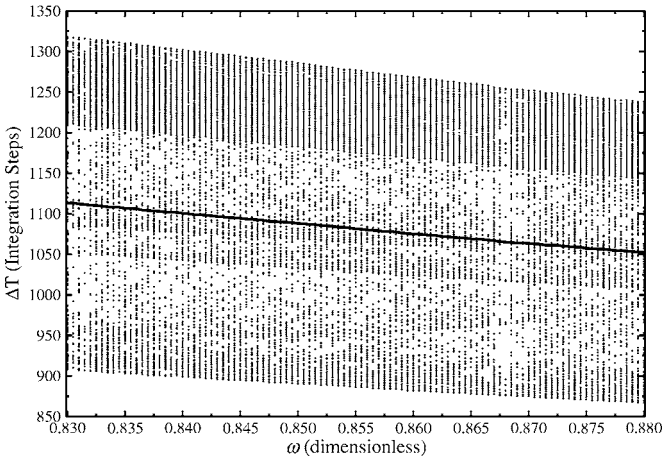

FIG. 1. This diagram shows the distribution of times (ΔT) between successive extrema as a function of the parameter mismatch ω. The model parameters are $\{p, q, r, s, \beta\}$ at $\{2.0\times10^{-4}, 1.0\times10^{-3}, 2.0\times10^{-5}, 9.7\times10^{-5}, 5.0\}$. The solid line that corresponds to the average value of the chaotic distribution, shows a definite variation for different values of ω.

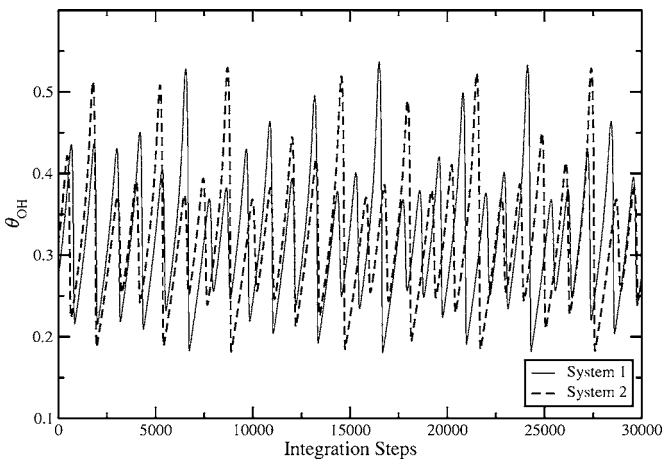

FIG. 2. Superimposed time series for the two chaotic oscillators with bidirectional coupling. The model parameters are $\{p, q, r, s, \beta, \omega_1, \omega_2\}$ at $\{2.0\times10^{-4}, 1.0\times10^{-3}, 2.0\times10^{-5}, 9.7\times10^{-5}, 5.0, 0.83, 0.88\}$, whereas the coupling constant is $\epsilon=5.0\times10^{-7}$. For this extremely small value of the coupling constant, the chaotic dynamics of the two systems evolve independent of each other.

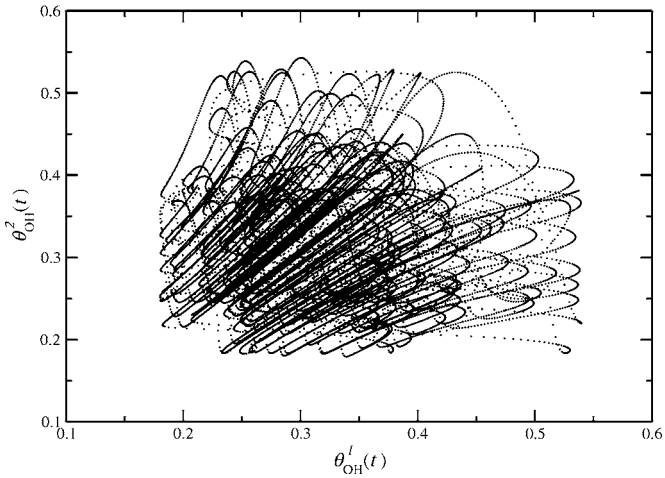

FIG. 3. Trajectories, corresponding to the time series of Fig. 2, in the phase space for the θ_{OH} variable of the two oscillators (system #1 and system #2). The resultant attractor is structureless, indicating that the two oscillators are in the domain of no synchronization.

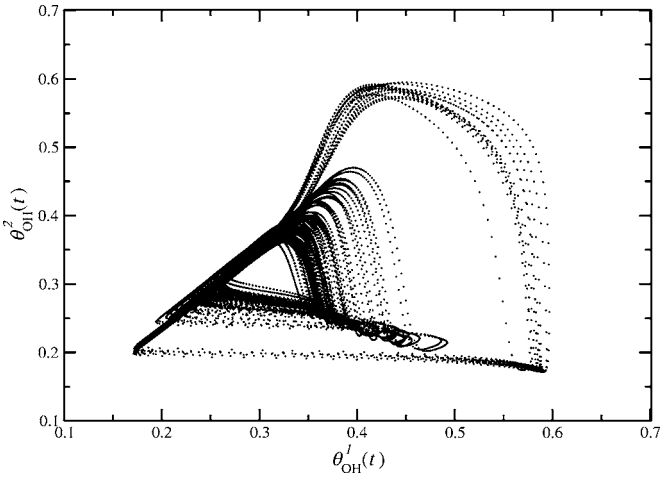

FIG. 5. Trajectories, corresponding to the time series of Fig. 4, in the phase space for the θ_{OH} variable of the two oscillators (system #1 and system #2). The resultant attractor is a closed curve, indicating that the two oscillators are located in the domain of phase synchronization.

For extremely weak coupling strengths, the two chaotic attractors oscillate independently. Figure 2 shows the independent chaotic evolution of the time series for the system variable θ_{OH}. The lack of cross correlation between the two chaotic times eries, a consequence of zero coupling, is more evident if one generates the θ^1_{OH} versus θ^2_{OH} plot, as shown in Fig. 3. The structureless attractor of Fig. 3 indicates that the two oscillators are located in the domain of "no synchronization."

As the coupling coefficient ϵ is increased, the two chaotic oscillators exhibit phase synchronization as depicted by the phase locking observed in the time series of Fig. 4. However, the amplitudes of the chaotic oscillations continue to evolve independently. Therefore, although there is no correlation in the amplitude domain, synchrony prevails in the frequency domain. The corresponding attractor of the coupled system, presented in Fig. 5 exhibiting phase synchronization,[30] reveals a closed curve typical for phase locked dynamics.

Augmenting the coupling strength (ϵ) further reveals the emergence of lag synchronization in the system dynamics. It needs to be emphasized that the bidirectional lag synchronization effect is hard to locate and needs not only a careful and systematic scan of the parameter mismatch (ω) but also an attentive analysis of the time series.[28,29] Figure 6 shows the chaotic time series of the coupled system exhibiting bidirectional lag synchronization. The constant time lag τ observed is an intrinsic property of the coupled system and can be varied, but only slightly, with suitable fine tuning of the system parameters (ω, ϵ, etc.). The $\theta^2_{OH}(t-\tau)$ versus $\theta^1_{OH}(t)$ plot, presented in Fig. 7, shows that the resultant attractor falls along the identity line consistent with the emergence of bidirectional lag synchronization.

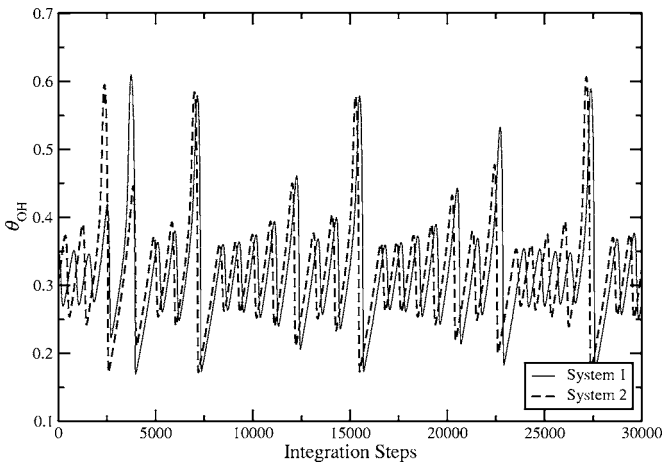

FIG. 4. The superimposed time series for the two chaotic oscillators with bidirectional coupling. The model parameters are $\{p, q, r, s, \beta, \omega_1, \omega_2\}$ at $\{2.0\times10^{-4}, 1.0\times10^{-3}, 2.0\times10^{-5}, 9.7\times10^{-5}, 5.0, 0.83, 0.88\}$, whereas the coupling constant is $\epsilon=12.3\times10^{-5}$. For this value of the coupling constant, the chaotic dynamics of the two systems are phase synchronized.

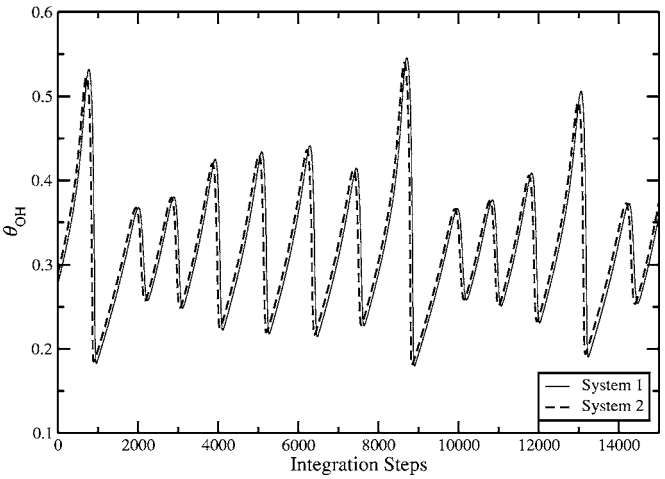

FIG. 6. The superimposed time series for the two chaotic oscillators with bidirectional coupling. The model parameters are $\{p, q, r, s, \beta, \omega_1, \omega_2\}$ at $\{2.0\times10^{-4}, 1.0\times10^{-3}, 2.0\times10^{-5}, 9.7\times10^{-5}, 5.0, 0.83, 0.88\}$, whereas the coupling constant is $\epsilon=5\times10^{-4}$. For this value of the coupling constant, the chaotic dynamics of the two systems exhibit lag synchronization.

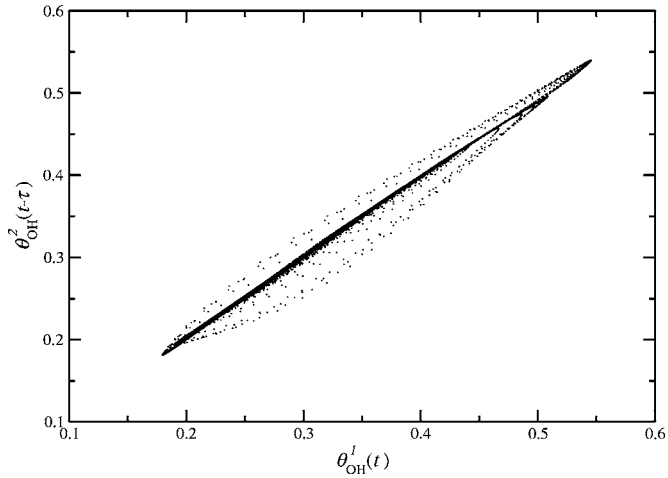

FIG. 7. Trajectories, corresponding to the time series of Fig. 6, in the phase space for the θ_{OH} variable of the two oscillators (system #1 and system #2). The resultant attractor, with an appropriate delay coordinate, falls along the line of identity, indicating that the two oscillators are in the domain of lag-synchronization.

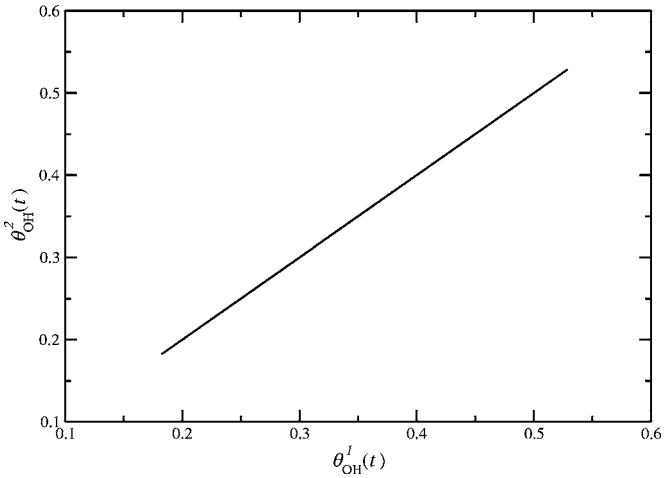

FIG. 9. Trajectories, corresponding to the time series of Fig. 8, in the phase space for the θ_{OH} variable of the two oscillators (system #1 and system #2). The resultant attractor, is sputtered along the line of identity, indicating that the two oscillators are in the domain of complete-synchronization.

Finally, for extremely large amplitudes of coupling constant, the chaotic oscillators, despite a small parameter mismatch, enter the domain of complete synchronization. This is evident, upon visual inspection of the superimposed chaotic time series of Fig. 8. Furthermore, the fact that $\theta^2_{OH}(t)$ versus $\theta^1_{OH}(t)$ attractor is sputtered along the line of identity (Fig. 9) confirms the inception of complete amplitude synchronization.

Apart from the qualitative visual evidence furnished by the superimposed time series and the projections of the appropriate attractors, a similarity function between the time series for the two coupled oscillators is calculated. This similarity function is a quantitative measure that has been used extensively to identify and subsequently classify the different domains of synchronization.[28,29] It is defined as

$$S(\tau) = \left(\frac{\langle [x_2(t+\tau) - x_1(t)]^2 \rangle}{[\langle x_1^2(t) \rangle \langle x_2^2(t) \rangle]^{1/2}} \right)^{1/2}, \tag{7}$$

and computes a time averaged difference between the two variables taken with the time shift τ. Figure 10 shows the similarity functions calculated using the time series for different coupling strengths. The curves labeled 6, 7 correspond to two instances when the two oscillators are located in the domain of no coupling and consequently no synchronization. For this scenario, the similarity function $S(\tau)$ fluctuates around an average numerical value of $\approx\sqrt{2}$.[28] Upon increasing the coupling constant, phase synchronization emerges depicted by the two curves labeled 4, 5. Lag synchronization follows and is illustrated by the similarity curves (labeled 2, 3) for which the numerical value of $S(\tau) \to 0$ for the corresponding lag time τ. Finally, the similarity function labeled 1

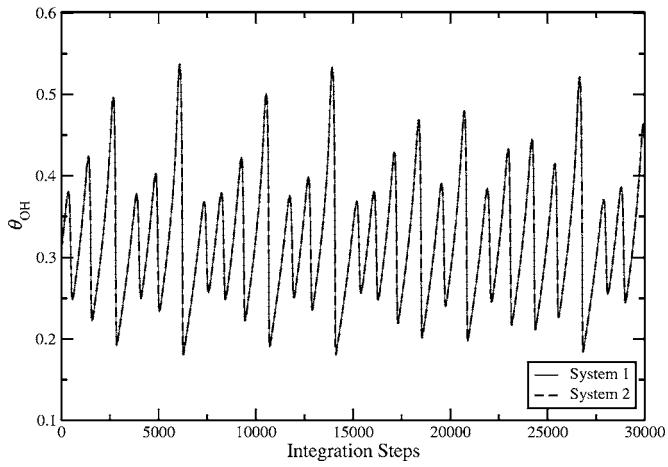

FIG. 8. The superimposed time series for the two chaotic oscillators with bidirectional coupling. The model parameters are $\{p, q, r, s, \beta, \omega_1, \omega_2\}$ at $\{2.0\times10^{-4}, 1.0\times10^{-3}, 2.0\times10^{-5}, 9.7\times10^{-5}, 5.0, 0.83, 0.88\}$, whereas the coupling constant is $\epsilon=0.5$. For this value of the coupling constant, the chaotic dynamics of the two systems exhibit complete amplitude synchronization.

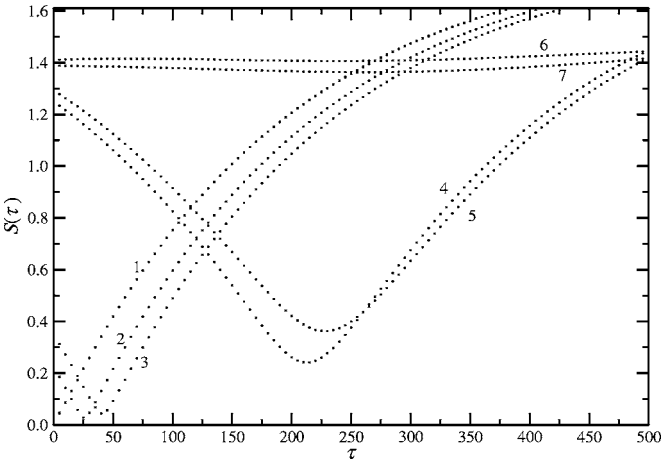

FIG. 10. Similarity functions $S(\tau)$ calculated for the different domains of synchronization observed upon monotonically varying the coupling constant ϵ. Curve 1, $\epsilon=0.5\rightarrow$amplitude synchronization. Curve 2, $\epsilon=12\times10^{-4}\rightarrow$lag synchronization. Curve 3, $\epsilon=8\times10^{-4}\rightarrow$lag synchronization. Curve 4, $\epsilon=13\times10^{-5}\rightarrow$phase synchronization. Curve 5, $\epsilon=12.3\times10^{-5}\rightarrow$phase synchronization. Curve 6, $\epsilon=2\times10^{-5}\rightarrow$no synchronization. Curve 7, $\epsilon=1\times10^{-5}\rightarrow$no synchronization.

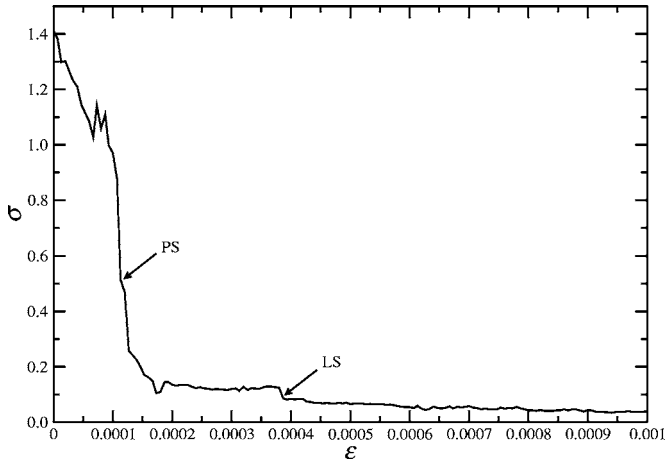

FIG. 11. The minima of the similarity function $S(\tau)$ plotted as a function of the coupling parameter ϵ. The model parameters for the two oscillators are $\{p, q, r, s, \beta, \omega_1, \omega_2\}$ at $\{2.0\times10^{-4}, 1.0\times10^{-3}, 2.0\times10^{-5}, 9.7\times10^{-5}, 5.0, 0.83, 0.88\}$. Also included are the approximate values for the transition points between the distinct domains of synchronization.

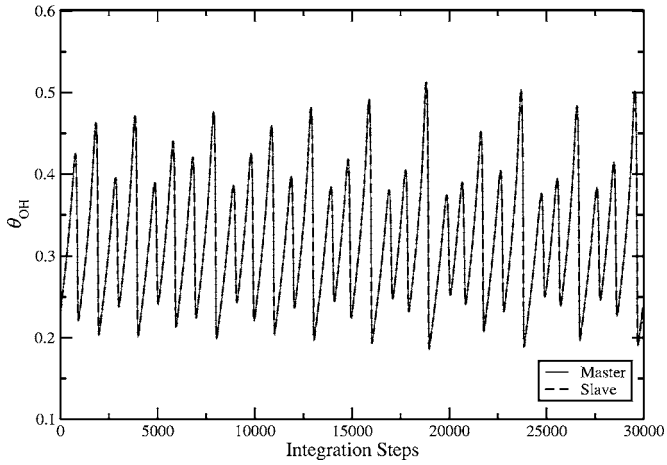

FIG. 12. The superimposed time series for the two oscillators with unidirectional coupling. The model parameters are $\{p, q, r, s, \beta\}$ at $\{2.0\times10^{-4}, 1.0\times10^{-3}, 2.0\times10^{-5}, 9.7\times10^{-5}, 5.0\}$, whereas the coupling parameters are $\epsilon=0.05$, $\tau_1=0.0$, $\tau_2=0.0$. For this case the chaotic dynamics of the two systems exhibit complete amplitude synchronization.

exhibits a monotonically increasing curve starting at the origin, typical for oscillators exhibiting complete synchronization. In Fig. 11, the minima (σ) of the similarity function $S(\tau)$ is plotted with respect to the coupling constant ϵ. It roughly divides the parameter region (in ϵ) into different domains corresponding to the nonsynchronous, phase synchronized, and lag synchronized states.

The results of this section indicate that for a suitable parameter mismatch, two chaotic oscillators subjected to a symmetric bidirectional coupling can exhibit different types of synchronization as the coupling strength is monotonically increased. This includes the transition from a state of no synchronization → phase synchronization → lag synchronization → complete amplitude synchronization. These different domains of synchronization are identified using standard diagnostic methods. The robustness of these numerical results is verified, augmenting the likelihood of detecting a similar transition sequence in real experimental situations.

IV. CHAOTIC SYNCHRONIZATION UNDER UNIDIRECTIONAL COUPLING

In this section, we present numerical results indicating the emergence of three different synchronization effects for appropriate unidirectional coupling functions. In contrast to the bidirectional scenario, coupling chaotic electrochemical oscillators unidirectionally yields a Master (M)-Slave (S) relationship between the two identical oscillators that can be described by the following set of coupled differential equations:

$$\dot{Y}^M = p(1-\theta_{\mathrm{OH}}^M-\theta_{\mathrm{O}}^M)-qY^M, \tag{8}$$

$$\dot{\theta}_{\mathrm{OH}}^M = Y^M(1-\theta_{\mathrm{OH}}^M-\theta_{\mathrm{O}}^M)-[\exp(-\beta\theta_{\mathrm{OH}}^M)+r]\theta_{\mathrm{OH}}^M + 2s\theta_{\mathrm{O}}^M(1-\theta_{\mathrm{OH}}^M-\theta_{\mathrm{O}}^M), \tag{9}$$

$$\dot{\theta}_{\mathrm{O}}^M = r\theta_{\mathrm{OH}}^M - s\theta_{\mathrm{O}}^M(1-\theta_{\mathrm{OH}}^M-\theta_{\mathrm{O}}^M), \tag{10}$$

$$\dot{Y}^S = p(1-\theta_{\mathrm{OH}}^S-\theta_{\mathrm{O}}^S)-qY^S, \tag{11}$$

$$\dot{\theta}_{\mathrm{OH}}^S = Y^S(1-\theta_{\mathrm{OH}}^S-\theta_{\mathrm{O}}^S)-[\exp(-\beta\theta_{\mathrm{OH}}^S)+r]\theta_{\mathrm{OH}}^S + 2s\theta_{\mathrm{O}}^S(1-\theta_{\mathrm{OH}}^S-\theta_{\mathrm{O}}^S) + \epsilon[\theta_{\mathrm{OH}}^M(t-\tau_1)-\theta_{\mathrm{OH}}^S(t-\tau_2)], \tag{12}$$

$$\dot{\theta}_{\mathrm{O}}^S = r\theta_{\mathrm{OH}}^S - s\theta_{\mathrm{O}}^S(1-\theta_{\mathrm{OH}}^S-\theta_{\mathrm{O}}^S). \tag{13}$$

The coupling term $\epsilon[\theta_{\mathrm{OH}}^M(t-\tau_1)-\theta_{\mathrm{OH}}^S(t-\tau_2)]$ is introduced in one of the Slave equations [Eq. (12)] and the different types of synchronizations are observed for an appropriate choice of time delays τ_1 and τ_2.

The first class of synchronization phenomena is observed when both τ_1 and τ_2 are chosen to be zero. This implies a coupling involving the present of the Master's dynamics and the present of the Slave behavior. Consequently, a transition scenario, starting from a domain of no synchronization → phase synchronization → complete synchronization is observed as the parameter ϵ, corresponding to the strength of the coupling constant, is switched ON and subsequently increased. This transition sequence is generic for the unidirectional coupling scenario and therefore has been exhaustively studied in a wide variety of systems.[8,10,15] Having observed the entire transition sequence, we present results from the final stage corresponding to the case of complete synchronization. Figure 12 shows the completely synchronized chaotic time series, whereas in Fig. 13, a projection of the attractor for the coupled system is presented. The system and the coupling parameters are furnished in the respective figure captions.

A. Lag synchronization under unidirectional coupling

For the observation of this class of synchronization effect, information from the past of the Master's dynamics is introduced in the present of the Slave dynamics.[15] This is

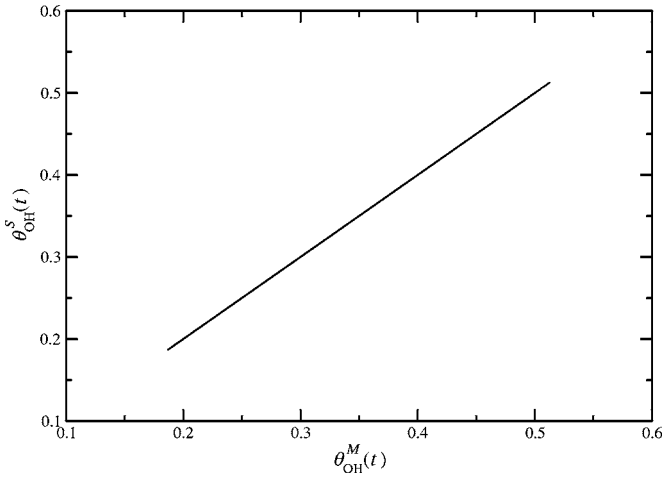

FIG. 13. Trajectories, corresponding to the time series of Fig. 12, in the phase space for the θ_{OH} variable of the two oscillators (system #1 and system #2). The resultant attractor is sputtered along the line of identity, indicating that the two oscillators are in the domain of complete synchronization.

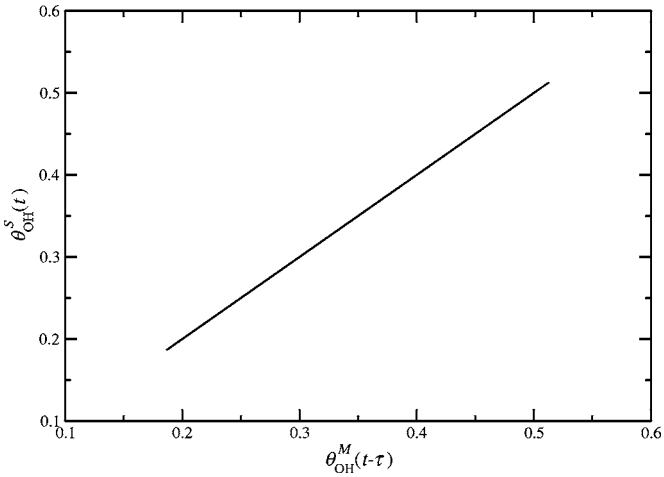

FIG. 15. Trajectories, corresponding to the time series of Fig. 14, in the phase space for the θ_{OH} variable of the two oscillators (system #1 and system #2). The resultant attractor, with an appropriate delay coordinate, falls along the line of identity, indicating that the two oscillators are in the domain of lag synchronization.

achieved by using an appropriate functional form for the coupling term in Eq. (12). Assigning a nonzero value to τ_1 and equating $\tau_2=0$, unidirectional lag synchronization phenomenon can be induced for a range of coupling amplitudes. Figure 14 shows the chaotic time series of the unidirectionally coupled oscillators exhibiting lag synchronization. An appropriate projection of the attractor for the coupled system as shown in Fig. 15 confirms this induction of unidirectional lag synchronization. In contrast to its bidirectional counterpart, which is extremely sensitive to the system and coupling parameters and consequently hard to detect, the unidirectional lag behavior is easy to locate since it is fairly robust. Another salient difference between the two lags (bidirectional and unidirectional) is that for the bidirectional scenario, the time lag τ between the two oscillators is intrinsic to the system/coupling parameters and hard to manipulate (vary). In comparison, for the unidirectional case, the time lag between the dynamics of the two oscillators is uniquely determined by the value of τ_1 inserted in Eq. (11). Therefore, contrary to the bidirectional lag, changing the time lag between the two oscillators is as trivial as modifying a coupling parameter. Finally, in our simulations, the emergence of the unidirectional lag phenomenon persists, even for large values of τ_1.

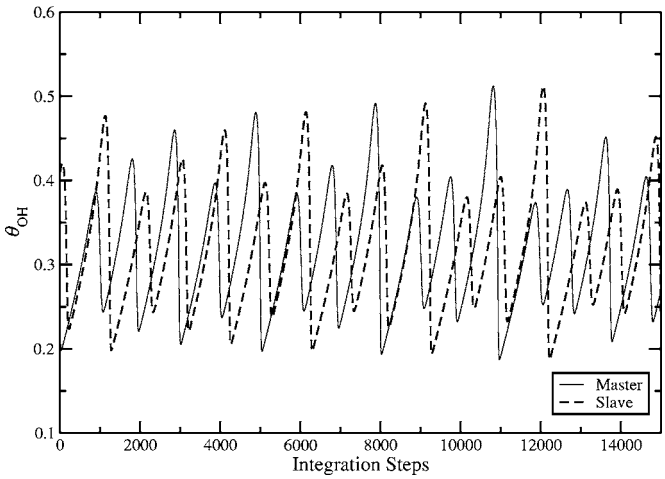

FIG. 14. The superimposed time series for the two oscillators with unidirectional coupling. The model parameters are $\{p, q, r, s, \beta\}$ at $\{2.0\times10^{-4}, 1.0\times10^{-3}, 2.0\times10^{-5}, 9.7\times10^{-5}, 5.0\}$, whereas the coupling parameters are $\epsilon=0.05$, $\tau_1=1250$, $\tau_2=0.0$. For this case the chaotic dynamics of the two systems exhibit lag synchronization.

B. Anticipation synchronization under unidirectional coupling

This fascinating class of synchronization, when conceived, allows the Slave oscillator to anticipate the chaotic evolution of the Master oscillator. Anticipation synchronization, when reported initially[31–33] created quite a stir in the field due to its possible applications and implications involving the prediction of chaotic behavior. To achieve anticipation synchronization, the coupling function introduced in Eq. (12) needs to be chosen such that $\tau_1=0$ and $\tau_2\neq0$. This functional form of the coupling term ensures a coupling between the present of Master's dynamics and the past of the Slave's dynamics. Successful synchronization is achieved when the past of the Slave dynamics is in synchrony with the present of the Master's. Consequently, the present of the Slave dynamics, a system observable, should be predicting/anticipating the Master's evolution.

Figure 16 shows the time series for the coupled system exhibiting anticipation synchronization. As is evident, visually, the dashed time trace corresponding to the chaotic Slave dynamics is ahead (anticipating) of the continuous time trace belonging to the Master. However, due to the positive Lyapunov exponent of the underlying chaotic dynamics, there exists an upper limit on the anticipation time observed. If coupling terms with still larger anticipation times are inserted, the model system is rendered numerically unstable.

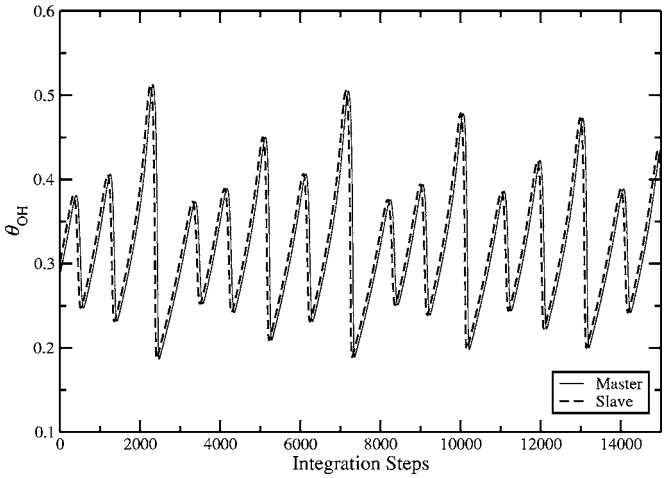

FIG. 16. The superimposed time series for the two oscillators with unidirectional coupling. The model parameters are $\{p, q, r, s, \beta\}$ at $\{2.0\times10^{-4}, 1.0\times10^{-3}, 2.0\times10^{-5}, 9.7\times10^{-5}, 5.0\}$, whereas the coupling parameters are $\epsilon=0.02$, $\tau_1=0.0$, $\tau_2=64$. For this case the chaotic dynamics of the two systems exhibit anticipation synchronization.

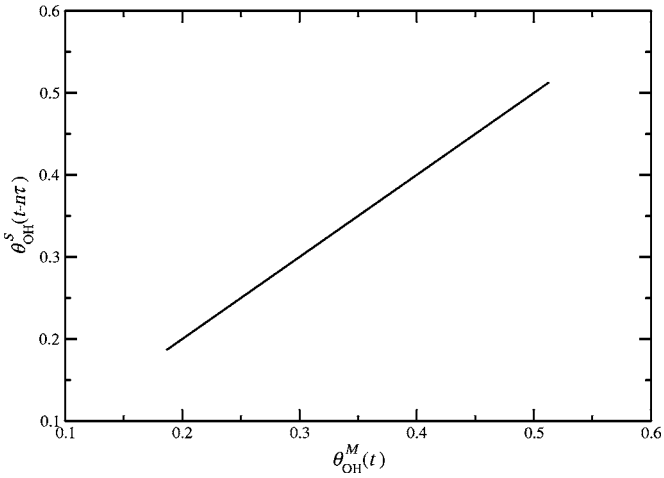

FIG. 18. Trajectories, corresponding to the time series of Fig. 17, in the phase space for the θ_{OH} variable of the two oscillators (system #1 and system #26). The resultant attractor, with appropriate delay coordinate ($n=25$), falls along the line of identity, indicating that the two oscillators are in the domain of anticipation-synchronization.

Unfortunately, for most chaotic systems, this maximum anticipation time is too small to envisage any potential applications.

To entertain any possibility of applying anticipation synchronization to relevant problems, one needs to circumvent this glaring drawback involving small anticipation times. A possible solution is to use a number of unidirectionally coupled chaotic oscillators (instead of two) in a linear chain configuration. Thereafter, by the definition of anticipation synchronization, each successive oscillator anticipates the evolution of the previous oscillator by a time τ_2. This sequential augmentation of the anticipation times ensures that the nth oscillator down the chain can anticipate the chaotic dynamics of the first oscillator by a time of $(n-1)\tau_2$. Figure 17, depicts the numerical results when 26 chaotic electrochemical oscillators are placed in a linear chain configuration and coupled accordingly, in a unidirectional fashion, to induce the anticipation effect. The time series of the oscillator #1 (solid line) and the oscillator #26 (dashed line) are superimposed. It clearly reveals the dramatic enhancement in anticipation times achieved. Moreover, an appropriate projection of the attractor for the coupled system, presented in Fig. 18, is distributed along the identity line and confirms the inception of anticipation synchronization. Therefore, a construction of a linear chain of chaotic oscillators seems to resolve the problem of small anticipation times.

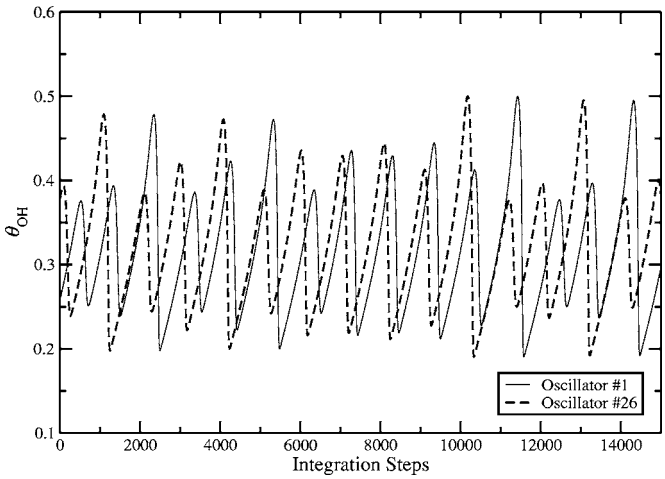

FIG. 17. The superimposed time series for the oscillator #1 (Master; continuous) and the oscillator #26 (Slave; dashed) with unidirectional coupling. The model parameters are $\{p, q, r, s, \beta\}$ at $\{2.0\times10^{-4}, 1.0\times10^{-3}, 2.0\times10^{-5}, 9.7\times10^{-5}, 5.0\}$, whereas the coupling parameters are $\epsilon=0.02$, $\tau_1=0.0$, $\tau_2=50$. In this case, the chaotic dynamics of the two systems exhibit enhanced anticipation synchronization by virtue of the linear chain configuration. The Slave dynamics now anticipate the Master's dynamics by a time of $\tau_2=25\times50=1250$.

V. CONCLUSIONS

We study the different types of synchronization phenomena observed when two chaotic electrochemical oscillators are subjected to bidirectional and unidirectional couplings. For the bidirectional case, a continuous transition sequence involving different classes of synchronization effects is observed as the coupling parameter is monotonically increased. For the induction of one of the elements of this transition sequence, namely the bidirectional lag synchronization, it is necessary to introduce an appropriate parameter mismatch between the two coupled chaotic oscillators. The inception of these different domains of synchronization is verified using both qualitative and quantitative techniques. Subsequently, distinct types of synchronization effects are studied for the case of unidirectional coupling. Using different functional forms of the coupling terms provokes contrasting synchronization phenomena. For one of these effects, namely anticipation synchronization, a serious drawback is encountered due to the underlying chaotic nature of the coupled dynamics. This drawback is subsequently overcome by substituting the two oscillator setup by an n oscillator linear chain. This present work is a composite of already reported synchronization phenomena in different model systems and new results. In particular, the results of Sec. IV A involving unidi-

rectional lag synchronization and the enhancement of anticipation times by virtue of sequential coupling (Sec. IV B) are novel findings for locally coupled chaotic oscillators.

Experimentally, a local bidirectional coupling can be implemented in experiments by simultaneously acquiring the two anodic currents and computing their mutual difference to evaluate the two coupling terms. These coupling terms would subsequently be used to perturb the two anodic voltages (system parameters) in order to observe the distinct bidirectional synchronization phenomena. This recipe gets naturally simplified for the unidirectional case. It involves measuring the anodic current from the master system and computing its difference from the anodic current of the slave system to obtain the appropriate coupling term. This coupling term would subsequently be superimposed on the anodic voltage of the slave electrode to obtain the different unidirectional synchronization phenomena. The possible application of our simulations to experiments and the robustness of the obtained results give credence to our belief that these distinct transition sequences and synchronization effects could be conceived in real experimental situations.

[1]T. Yamada and H. Fujisaksa, Prog. Theor. Phys. **70**, 1240 (1983).
[2]T. Yamada and H. Fujisaksa, Prog. Theor. Phys. **72**, 885 (1984).
[3]V. S. Afraimovich, N. N. Verichev, and M. I. Rabinovich, Radiophys. Quantum Electron. **29**, 795 (1986).
[4]L. M. Pecora and T. L. Carroll, Phys. Rev. Lett. **64**, 821 (1990).
[5]L. M. Pecora and T. L. Carroll, Phys. Rev. A **44**, 2374 (1991).
[6]S. K. Han, C. Kurrer, and Y. Kuramoto, Phys. Rev. Lett. **75**, 3190 (1995).
[7]M. A. Harrison, Y-Ch. Lai, and R. D. Holt, Phys. Rev. E **63**, 051905 (2001).
[8]K. S. Thornburg, Jr., M. Möller, R. Roy, T. W. Carr, R. D. Li, and T. Erneux, Phys. Rev. E **55**, 3865 (1997).
[9]P. Ashwin, J. R. Terry, K. S. Thornburg, Jr., and R. Roy, Phys. Rev. E **58**, 7186 (1998).
[10]C. Masoller, Hugo L. D. de S. Cavalcante, and J. R. Rios Leite, Phys. Rev. E **64**, 037202 (2001).
[11]I. Z. Kiss, V. Gaspar, and J. L. Hudson, J. Phys. Chem. B **104**, 7554 (2000).
[12]A. Pikovsky, M. Rosenblum, and J. Kurths, *Synchronization A Universal Concept in Nonlinear Sciences* (Cambridge University Press, Cambridge, 2001).
[13]S. Strogatz, *Sync: The Emerging Science of Spontaneous Order* (Hyperion, New York, 2003).
[14]E. Mosekilde, Y. Maistrenko, and D. Postnov, *Chaotic Synchronization Applications to Living Systems* (World Scientific, Singapore, 2002).
[15]S. Boccaletti, J. Kurths, G. Osipov, D. L. Valladares, and C. S. Zhou, Phys. Rep. **366**, 1 (2002).
[16]M. R. Bassett and J. L. Hudson, J. Phys. Chem. **93**, 6963 (1989).
[17]Y. Wang, J. L. Hudson, and N. I. Jaeger, J. Electrochem. Soc. **137**, 485 (1990).
[18]J. L. Hudson and M. R. Bassett, Rev. Chem. Eng. **7**, 109 (1991).
[19]H. D. Dewald, P. Parmananda, and R. W. Rollins, J. Electroanal. Chem. Interfacial Electrochem. **306**, 297 (1991).
[20]H. D. Dewald, P. Parmananda, and R. W. Rollins, J. Electrochem. Soc. **140**, 1969 (1993).
[21]W. Wang, I. Z. Kiss, and J. L. Hudson, Chaos **10**, 248 (2000).
[22]W. Wang, I. Z. Kiss, and J. L. Hudson, Phys. Rev. Lett. **86**, 4954 (2001).
[23]M. G. Rosenblum, A. S. Pikovsky, J. Kurths, G. V. Osipov, I. Z. Kiss, and J. L. Hudson, Phys. Rev. Lett. **89**, 264102 (2002).
[24]I. Z. Kiss, Y. M. Zhai, and J. L. Hudson, Science **296**, 1676 (2002).
[25]I. Z. Kiss, Y. Zhai, and J. L. Hudson, Phys. Rev. Lett. **88**, 238301 (2002).
[26]J. B. Talbot and R. A. Oriani, Electrochim. Acta **30**, 1277 (1985).
[27]J. K. McCoy, P. Parmananda, R. W. Rollins, and A. J. Markworth, J. Mater. Res. **8**, 4596 (1993).
[28]M. G. Rosenblum, A. S. Pikovsky, and J. Kurths, Phys. Rev. Lett. **78**, 4193 (1997).
[29]S. Boccaletti and D. L. Valladeras, Phys. Rev. E **62**, 7497 (2000).
[30]I. Z. Kiss and J. L. Hudson, Phys. Rev. E **64**, 046215 (2001).
[31]H. U. Voss, Phys. Rev. E **61**, 5115 (2000).
[32]H. U. Voss, Phys. Rev. Lett. **87**, 014102 (2001).
[33]C. Masoller, Phys. Rev. Lett. **86**, 2782 (2001).